

Structure and Optical Properties of Thermochromic Schiff Bases. Charge Transfer Interaction and Proton Transfer in the *N*-Tetrachlorosalicylideneaniline and *N*-Tetrachlorosalicylidene-1-pyrenylamine Crystals

Tamotsu INABE,* Isabelle GAUTIER-LUNEAU,^{†,††} Naomi HOSHINO,^{††} Kaoru OKANIWA,[†] Hiroshi OKAMOTO, Tadaoki MITANI, Umpei NAGASHIMA, and Yusei MARUYAMA*

Institute for Molecular Science, Myodaiji, Okazaki 444

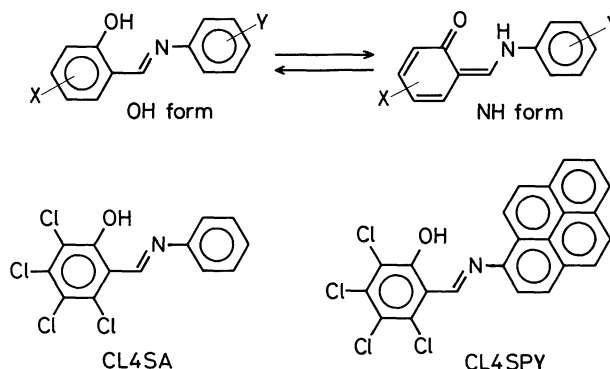
[†] Graduate University for Advanced Studies and Institute for Molecular Science, Myodaiji, Okazaki 444

(Received June 22, 1990)

Two kinds of *N*-salicylideneaniline derivatives, *N*-tetrachlorosalicylideneaniline (CL4SA) and *N*-tetrachlorosalicylidene-1-pyrenylamine (CL4SPY), have been prepared and subjected to structural and optical studies in the crystalline state. A thermochromic-type behavior of the former crystal has been observed as a shift of the absorption edge, while that of the latter crystal is much less pronounced. Fairly short O–H...N hydrogen bonds have been found in both compounds through crystallographic studies, which may be mainly due to a steric effect of chlorine substituents. The difference in the proton transfer behavior of CL4SA and CL4SPY should presumably be caused by an intermolecular charge-transfer interaction in the latter crystal.

N-Salicylideneaniline derivatives have been known to show a self-isomerization induced by an intramolecular proton transfer from the hydroxyl oxygen to the imine nitrogen through the O–H...N hydrogen bond. Since this type of proton transfer process involves a π -electron configurational change, the two isomers produced by the proton transfer have different electronic states. Sometimes, this self-isomerization is observed in the crystalline state as thermochromism or photochromism.¹⁾ We have recently carried out structural and optical studies of the thermochromism of *N,N'*-disalicylidene-*p*-phenylenediamine (BSP) crystals.²⁾ In this crystal the planar BSP molecules are stacked one-dimensionally with a short interplanar spacing (3.29 Å at room temperature and 3.26 Å at 108 K³⁾). These relatively short distances suggest that some intermolecular interaction operates in the crystal; we have assigned it to a charge-transfer interaction.

We are particularly interested in the case where the intermolecular interaction is sufficiently strong that the electronic properties of the crystal may be modulated by proton motion. This coupling between protons and electrons may be utilized for designing materials which have novel types of electronic properties.⁴⁾ From this point of view, the introduction of a sufficiently strong charge-transfer interaction into the *N*-salicylideneaniline system is supposed to be an effective approach. In this paper we report the synthesis of the title compounds, in which an *o*-chloranil-like acceptor portion and aromatic-amine-like donor portions are produced when the proton transfers to the imine nitrogen (NH form). The structural and optical properties of the CL4SA and



CL4SPY crystals are also described with emphasis on the nature of their fairly strong hydrogen bonds.

Experimental

Materials. CL4SA was prepared by the condensation of tetrachlorosalicylaldehyde and aniline in refluxed methanol, and was recrystallized from benzene. Tetrachlorosalicylaldehyde was synthesized from tetrachlorophthalic anhydride by following a method reported by Heaney et al.⁵⁾ Needle-like single crystals of CL4SA were obtained by slow evaporation of the benzene solution.

CL4SPY was prepared by the condensation of tetrachlorosalicylaldehyde and 1-pyrenylamine in the same manner as CL4SA, and was recrystallized from chlorobenzene. Needle-like single crystals of CL4SPY were grown by slow cooling of a chlorobenzene solution.

Optical Measurements. The infrared and visible absorption as well as the emission spectra were measured using single-crystal specimens and the same methods as reported before.²⁾

X-Ray Structure Analyses. The data-collection conditions and the crystal data are summarized in Table 1. In both cases, the measurements were carried out at room temperature with graphite monochromatized MoK α radiation ($\lambda=0.71073$ Å). The intensities of the three standards used (monitored every 100 data measurements) remained constant within 3% for both crystals.

^{††} Present address: LIESG, ENSEEG, Domaine Universitaire BP75, 38402 Saint-Martin D'Herès, France.

^{†††} Present address: Department of Chemistry, Faculty of Science, Hokkaido University, Sapporo 060.

Table 1. Data-Collection Conditions and Crystal Data

	CL4SA	CL4SPY
Diffractometer	Rigaku AFC-5	Rigaku AFC-5R
2 θ range	<60°	<50°
Range of h , k , and l	$-19 \leq h \leq 19$ $0 \leq k \leq 34$ $0 \leq l \leq 5$	$-17 \leq h \leq 17$ $0 \leq k \leq 17$ $0 \leq l \leq 9$
Scan width/°	$1.2 + 0.5 \tan \theta$	$1.2 + 0.5 \tan \theta$
Scan mode	θ -2 θ	θ -2 θ
Scan rate/° min ⁻¹	3	4
Number of unique reflections measured	3995	3447
Number of independent reflections observed ($ F_o > 3\sigma(F_o)$)	1021	1280
Background count time/sec	8—21.4	5—14.9
Lattice parameter measurement		
2 θ range/°	$20 < 2\theta < 30$	$20 < 2\theta < 27$
Number of reflections	25	25
Chemical formula	C ₁₃ H ₇ NOCl ₄	C ₂₃ H ₁₁ NOCl ₄
Molecular weight	335.017	459.159
Crystal color	Orange	Dark red
Crystal size/mm	0.1×0.1×0.7	0.06×0.06×0.5
Crystal system	Monoclinic	Monoclinic
Space group	$P2_1/a$	$P2_1/a$
$a/\text{\AA}$	14.117(7)	15.135(3)
$b/\text{\AA}$	24.240(9)	15.298(4)
$c/\text{\AA}$	3.898(2)	8.197(2)
β/deg	93.62(5)	100.05(2)
$V/\text{\AA}^3$	1331.2(10)	1868.9(7)
Z	4	4
$D_c/\text{g cm}^{-3}$	1.672	1.633
$\mu(\text{Mo K}\alpha)/\text{cm}^{-1}$	8.81	6.51
R	0.046	0.035
R_w	0.063	0.034
Weighting factor (g) [$w^{-1} = \sigma^2 + (gF)^2$]	0.040	0.015

Table 2. Atomic Parameters for CL4SA ($\times 10^4$)

Atom	x	y	z	$B_{\text{eq}}/\text{\AA}^2$ ^{a)}
Cl(1)	10622 (1)	1092 (1)	-1198 (6)	5.2
Cl(2)	9047 (2)	384 (1)	2012 (5)	5.0
Cl(3)	7086 (1)	903 (1)	3217 (5)	4.6
Cl(4)	6693 (1)	2132 (1)	1223 (5)	4.7
O(5)	10027 (3)	2190 (2)	-3079 (13)	4.2
N(6)	8904 (4)	2996 (2)	-3685 (14)	3.5
C(7)	8465 (4)	2160 (3)	-1068 (16)	2.7
C(8)	9350 (4)	1912 (3)	-1593 (17)	3.2
C(9)	9526 (5)	1366 (3)	-588 (17)	3.2
C(10)	8828 (4)	1060 (3)	893 (17)	3.4
C(11)	7954 (4)	1296 (3)	1430 (16)	2.8
C(12)	7775 (4)	1837 (3)	523 (16)	3.0
C(13)	8273 (5)	2717 (3)	-2138 (17)	3.5
C(14)	8755 (5)	3540 (3)	-4926 (17)	3.3
C(15)	7869 (5)	3788 (3)	-5376 (19)	4.2
C(16)	7811 (5)	4321 (3)	-6600 (20)	4.5
C(17)	8608 (6)	4620 (3)	-7334 (20)	4.7
C(18)	9476 (6)	4360 (4)	-6960 (22)	5.3
C(19)	9563 (5)	3827 (3)	-5740 (19)	4.3

a) $B_{\text{eq}} = 4/3 \sum_i \sum_j \beta_{ij} a_i a_j$.

Both crystal structures were solved by a direct method,⁶⁾ and the positions of all hydrogen atoms were determined from difference synthesis maps. A block-diagonal least-squares technique (UNICS III⁷⁾) with anisotropic thermal

Table 3. Atomic Parameters for CL4SPY ($\times 10^4$)

Atom	x	y	z	$B_{\text{eq}}/\text{\AA}^2$
Cl(1)	680 (1)	-2937 (1)	6206 (2)	4.6
Cl(2)	2654 (1)	-2721 (1)	7983 (2)	4.4
Cl(3)	3760 (1)	-1088 (1)	7303 (2)	4.7
Cl(4)	2839 (1)	399 (1)	5040 (2)	4.3
O(5)	0 (2)	-1460 (2)	4144 (4)	3.8
N(6)	99 (2)	-24 (3)	2645 (5)	2.9
C(7)	1332 (3)	-596 (3)	4579 (6)	2.5
C(8)	841 (3)	-1358 (3)	4863 (6)	3.0
C(9)	1274 (3)	-2009 (3)	5919 (6)	2.7
C(10)	2157 (3)	-1911 (3)	6679 (6)	2.9
C(11)	2651 (3)	-1171 (3)	6413 (6)	2.9
C(12)	2237 (3)	-527 (3)	5378 (6)	2.8
C(13)	916 (3)	55 (3)	3439 (6)	3.1
C(14)	-334 (3)	590 (3)	1488 (6)	2.9
C(15)	91 (3)	1340 (3)	1065 (7)	3.6
C(16)	-336 (3)	1930 (3)	-67 (7)	3.9
C(17)	-1223 (3)	1814 (3)	-784 (6)	3.0
C(18)	-1676 (3)	1051 (3)	-378 (6)	2.6
C(19)	-1223 (3)	423 (3)	743 (5)	2.4
C(20)	-1703 (4)	2426 (3)	-1957 (6)	3.8
C(21)	-2583 (4)	2316 (3)	-2585 (6)	3.9
C(22)	-3064 (3)	1572 (3)	-2169 (6)	3.2
C(23)	-3982 (4)	1448 (4)	-2796 (7)	5.1
C(24)	-4424 (3)	703 (4)	-2408 (7)	5.0
C(25)	-3971 (4)	65 (4)	-1392 (7)	4.3
C(26)	-3056 (3)	167 (3)	-725 (6)	3.1
C(27)	-2571 (3)	-464 (3)	358 (6)	3.3
C(28)	-1705 (3)	-349 (3)	1060 (6)	3.2
C(29)	-2596 (3)	930 (3)	-1090 (6)	2.8

parameters for non-hydrogen atoms and isotropic for hydrogen atoms was employed for the structure refinement.

Results

Structures. The atomic parameters of CL4SA and CL4SPY obtained by X-ray analyses are listed in Tables 2 and 3, respectively. Both molecular structures are shown in Fig. 1; the bond lengths and angles are listed in Table 4. The dihedral angle between two aromatic groups connected by the azomethine group is 15° for CL4SA and 2.3° for CL4SPY. These values are much smaller compared with that of *N,N'*-disalicylidene-1,6-pyrenediamine, DSPY (42°), in which proton transfer is suppressed.⁹⁾

The most noticeable point commonly observed for both compounds is the quite short distance of O(5)⋯N(6) (2.517(7) Å for CL4SA and 2.534(7) Å for CL4SPY), which form the hydrogen bond. The corresponding distances are in the range between 2.58

and 2.62 Å for other *N*-salicylideneanilines.^{2,3,9,10)} The O(5)–C(8) bond lengths (1.332(8) Å for CL4SA and 1.316(5) Å for CL4SPY) are also shorter than those of BSP, DSPY, 2-chloro-*N*-salicylideneaniline,⁹⁾ and *N*-(5-chlorosalicylidene)aniline,¹⁰⁾ in which the values are in the range between 1.350 and 1.365 Å. This contraction obviously indicates that there exists a resonance contribution from the quinonoid structure, which is produced when a proton transfers from the hydroxyl oxygen to the imine nitrogen. A corresponding alternation of the bond lengths of the benzene ring expected for a quinonoid structure has been observed for both compounds.

The crystal structures of CL4SA and CL4SPY are shown in Figs. 2(a) and (b), respectively. The CL4SA molecules are translationally stacked along the *c*-axis; the interplanar distances are 3.44 Å between the tetrachlorophenol rings and 3.64 Å between the benzene rings of the aniline side. On the other hand, the

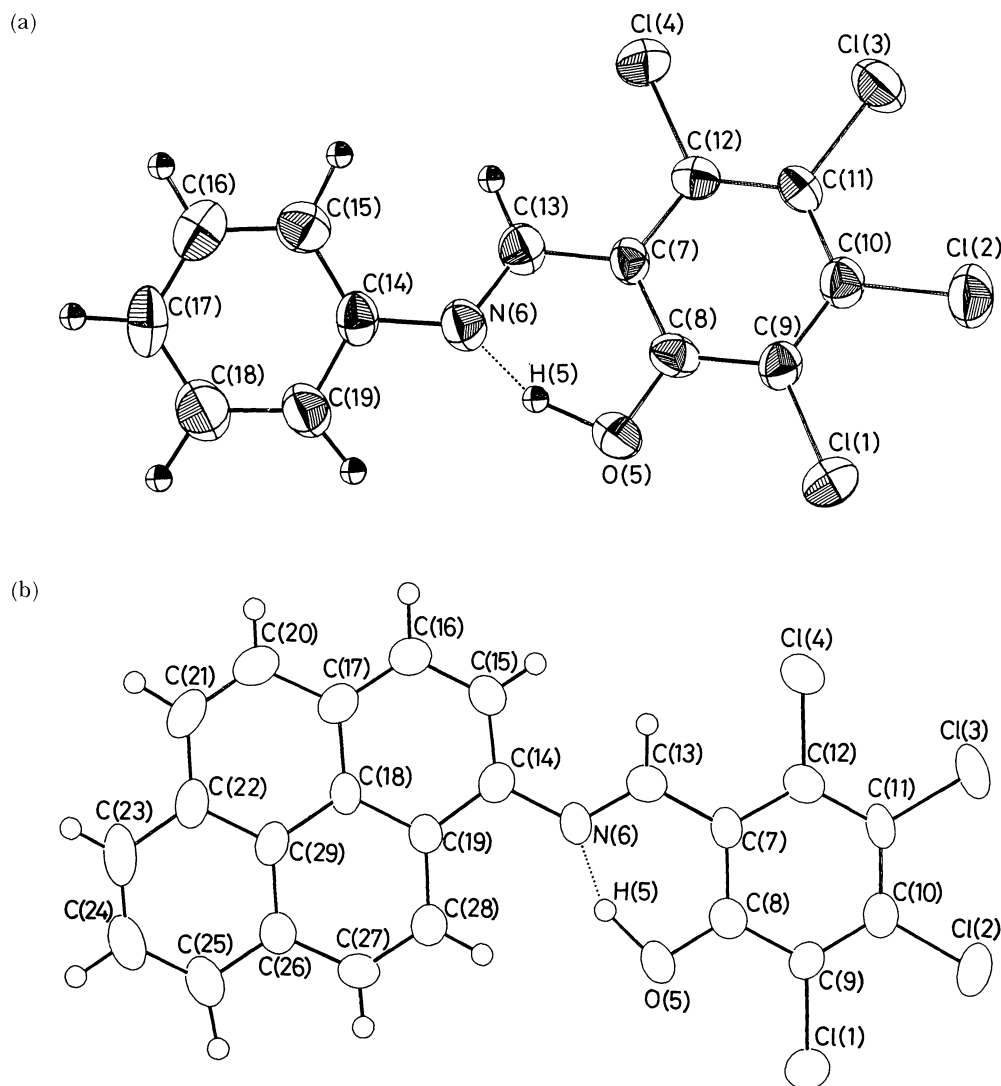


Fig. 1. ORTEP drawing¹⁶⁾ of CL4SA (a) and CL4SPY (b) showing the atom numbering scheme.

Table 4. Bond Lengths and Angles of CL4SA and CL4SPY

	CL4SA	CL4SPY		CL4SA	CL4SPY
Distance	<i>l</i> /Å	<i>l</i> /Å	C(7)–C(8)–C(9)	120.3(6)	118.8(4)
Cl(1)–C(9)	1.715(7)	1.719(5)	Cl(1)–C(9)–C(8)	118.2(5)	118.1(3)
Cl(2)–C(10)	1.718(7)	1.721(5)	Cl(1)–C(9)–C(10)	121.4(5)	121.1(4)
Cl(3)–C(11)	1.731(7)	1.715(4)	C(8)–C(9)–C(10)	120.3(6)	120.8(4)
Cl(4)–C(12)	1.724(7)	1.732(5)	Cl(2)–C(10)–C(9)	119.6(5)	119.0(4)
O(5)–C(8)	1.332(8)	1.316(5)	Cl(2)–C(10)–C(11)	120.1(5)	119.6(3)
N(6)–C(13)	1.298(9)	1.298(6)	C(9)–C(10)–C(11)	120.2(6)	121.4(4)
N(6)–C(14)	1.414(9)	1.413(6)	Cl(3)–C(11)–C(10)	119.5(5)	120.3(4)
C(7)–C(8)	1.412(9)	1.423(7)	Cl(3)–C(11)–C(12)	120.2(5)	121.0(4)
C(7)–C(12)	1.422(9)	1.415(6)	C(10)–C(11)–C(12)	120.3(6)	118.6(4)
C(7)–C(13)	1.435(9)	1.434(7)	Cl(4)–C(12)–C(7)	118.7(5)	118.8(4)
C(8)–C(9)	1.399(9)	1.405(6)	Cl(4)–C(12)–C(11)	120.2(5)	119.2(3)
C(9)–C(10)	1.387(9)	1.380(6)	C(7)–C(12)–C(11)	121.0(6)	122.0(4)
C(10)–C(11)	1.388(9)	1.394(7)	N(6)–C(13)–C(7)	120.2(6)	122.3(4)
C(11)–C(12)	1.380(9)	1.378(7)	N(6)–C(14)–C(15)	124.1(6)	122.4(4)
C(14)–C(15)	1.390(10)	1.389(7)	N(6)–C(14)–C(19)	116.0(6)	118.0(4)
C(14)–C(19)	1.390(10)	1.400(6)	C(15)–C(14)–C(19)	120.0(7)	119.6(4)
C(15)–C(16)	1.378(11)	1.373(7)	C(14)–C(15)–C(16)	118.9(7)	121.8(4)
C(16)–C(17)	1.382(12)	1.379(7)	C(15)–C(16)–C(17)	122.1(7)	120.8(5)
C(17)–C(18)	1.378(12)	1.422(7)	C(16)–C(17)–C(18)	118.0(7)	118.6(4)
C(18)–C(19)	1.379(11)	1.420(6)	C(17)–C(18)–C(19)	121.6(8)	120.6(4)
C(17)–C(20)	—	1.444(7)	C(16)–C(17)–C(20)	—	122.7(5)
C(18)–C(29)	—	1.425(6)	C(18)–C(17)–C(20)	—	118.7(4)
C(19)–C(28)	—	1.436(7)	C(17)–C(18)–C(29)	—	119.2(4)
C(20)–C(21)	—	1.352(7)	C(19)–C(18)–C(29)	—	120.2(4)
C(21)–C(22)	—	1.424(8)	C(14)–C(19)–C(18)	—	118.5(4)
C(22)–C(23)	—	1.408(7)	C(14)–C(19)–C(28)	—	123.5(4)
C(22)–C(29)	—	1.423(7)	C(18)–C(19)–C(28)	—	118.1(4)
C(23)–C(24)	—	1.387(8)	C(17)–C(20)–C(21)	—	121.4(5)
C(24)–C(25)	—	1.385(8)	C(20)–C(21)–C(22)	—	121.3(5)
C(25)–C(26)	—	1.407(7)	C(21)–C(22)–C(23)	—	122.3(5)
C(26)–C(27)	—	1.426(7)	C(21)–C(22)–C(29)	—	118.7(4)
C(26)–C(29)	—	1.417(7)	C(23)–C(22)–C(29)	—	119.1(5)
C(27)–C(28)	—	1.348(7)	C(22)–C(23)–C(24)	—	120.8(5)
O(5)–H(5)	1.18 (9)	1.17 (6)	C(23)–C(24)–C(25)	—	120.6(5)
N(6)···H(5)	1.38 (9)	1.44 (7)	C(24)–C(25)–C(26)	—	120.4(5)
			C(25)–C(26)–C(27)	—	122.1(5)
Angle	$\theta/^\circ$	$\theta/^\circ$	C(25)–C(26)–C(29)	—	119.8(4)
C(13)–C(6)–C(14)	123.6(6)	124.4(4)	C(27)–C(26)–C(29)	—	118.1(4)
C(8)–C(7)–C(12)	117.8(6)	118.5(4)	C(26)–C(27)–C(28)	—	122.2(5)
C(8)–C(7)–C(13)	120.7(6)	119.5(4)	C(19)–C(28)–C(27)	—	121.2(4)
C(12)–C(7)–C(13)	121.5(6)	121.9(4)	C(22)–C(29)–C(26)	—	119.3(4)
O(5)–C(8)–C(7)	120.8(6)	121.0(4)	C(18)–C(29)–C(22)	—	120.6(4)
C(5)–C(8)–C(9)	118.8(6)	120.2(4)	C(18)–C(29)–C(26)	—	120.1(4)

CL4SPY molecules are stacked with an alternating orientation. As shown in Fig. 2(c), this stacking mode leads to an effective intermolecular overlapping of the donor and acceptor parts. Consequently, the interplanar distances between the mean planes of the entire molecule are short, i.e., 3.37 and 3.39 Å, and there are several short interatomic distances between stacked molecules (Fig. 2(c)). The intermolecular contacts in CL4SA are longer than the sum of the van der Waals radii, except for Cl(2)···C(11) (3.489(7) Å).

Optical Properties. The polarized infrared spectra of the CL4SA single crystal at room temperature are shown in Fig. 3(a). An extremely broad band centered at ca. 2700 cm^{−1} is observed when the polarization is perpendicular to the *c*-axis. Since the hump at

3030 cm^{−1} is undoubtedly assigned to the CH stretching mode, this broad molecular in-plane component is assignable to the OH stretching mode. Compared with BSP and DSPY, the intensity is considerably weak, although the position and the half width (ca. 600 cm^{−1}) is comparable. Figure 3(b) shows the infrared spectra of the CL4SPY single crystal at room temperature. A broad OH stretching band was observed at ca. 2600 cm^{−1}. The half width is ca. 700 cm^{−1}, which is slightly larger than that of CL4SA. The intensity seems to be even weaker, compared with the normalized intensity of the CH stretching mode at 3030 cm^{−1}.

Figure 4(a) shows the absorption spectra of the CL4SA single crystal at various temperatures. The

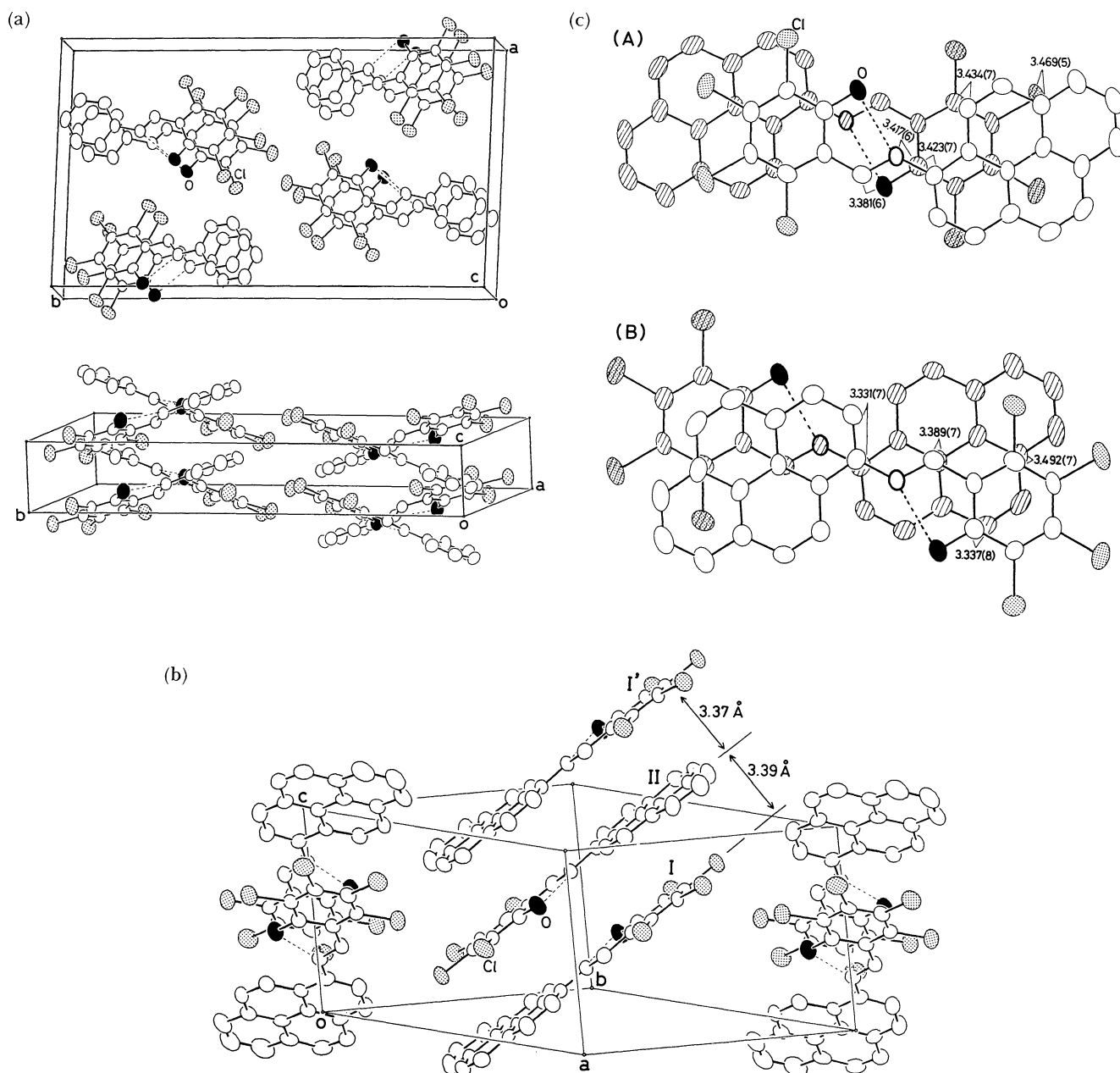


Fig. 2. Crystal structures of CL4SA (a) and CL4SPY (b); symmetry code, I (x, y, z), II ($1-x, 1-y, 1-z$), I' ($x, y, 1+z$), and molecular overlapping between the CL4SPY molecules, I and II (A) and II and I' (B) and some short interatomic distances (Å) (c).

thermochromic-type behavior is observed as a shift of the absorption edge with temperature. This behavior represents a different type of thermochromism from that ordinarily observed for other *N*-salicylideneanilines. For example, in BSP, a new band appeared in the lower-energy region grows with increasing temperature.²⁾ The emission spectra of CL4SA (Fig. 4) show a Stokes shift (0.35 eV at 6 K and 0.25 eV at 300 K from the absorption edge). No noticeable change of the band profile was observed with changing temperature.

The visible region absorption spectra of the CL4SPY

single crystal is shown in Fig. 4(b). Though a shift in the absorption edge due to a temperature change was observed, the energy of a shift was about half that observed in CL4SA over the same temperature range. On the other hand, the emission spectra showed a complicated change with the temperature. At 8 K, five peaks were observed at 2.04, 1.99, 1.85, 1.70, and 1.55 eV. With increasing temperature, the first peak merged into the second peak. The other three peaks, which are equally separated by 0.15 eV, shifted slightly towards higher energy by 132 K, then merged into one band at 1.83 eV. The intensities decreased rather

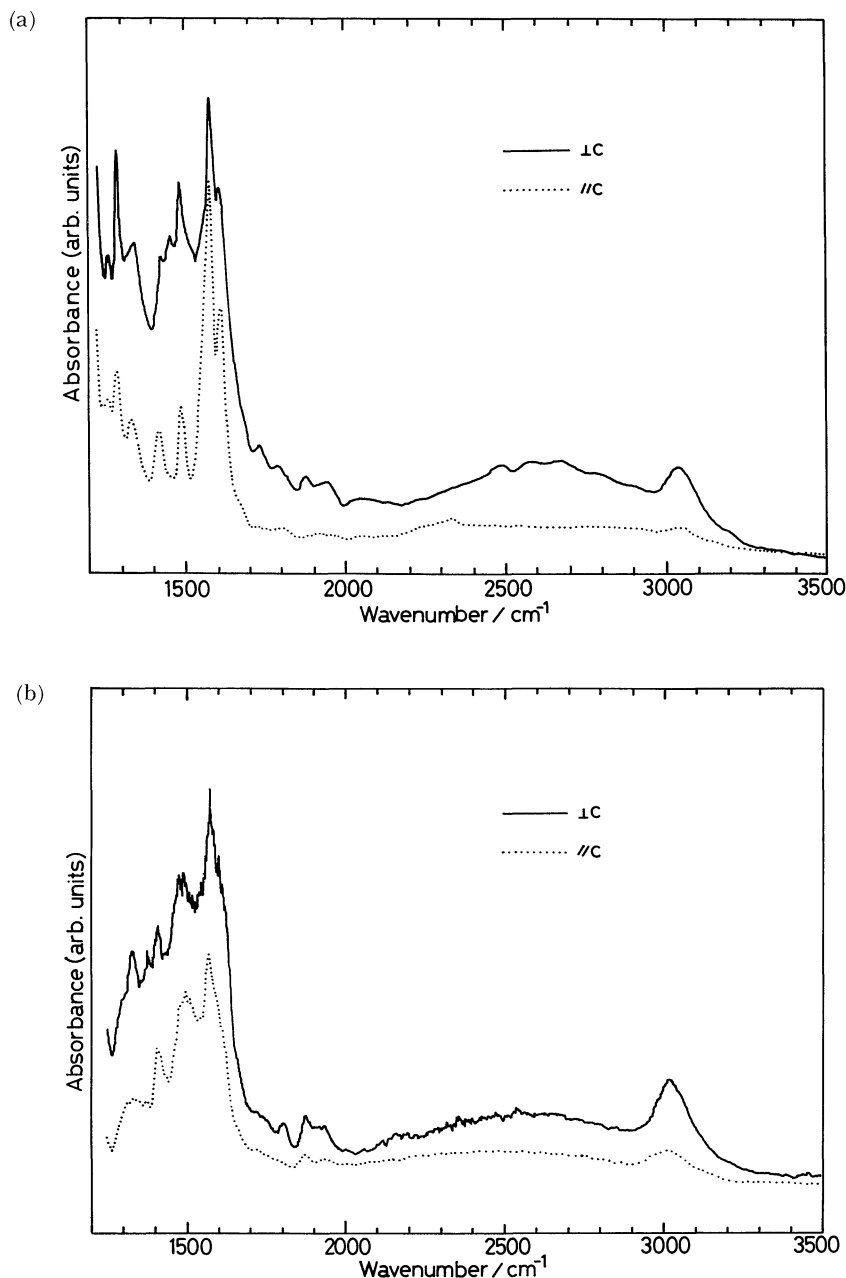


Fig. 3. Single-crystal infrared spectra for CL4SA (a) and CL4SPY (b) at room temperature.

rapidly with increasing temperature to 74 K, then decreased gradually.

Discussion

When the O...N distance is short enough to make the energy difference and the barrier height appreciably small, in reference to the thermal energy, the proton transfer is thermally allowed in *N*-salicylideneanilines. In both CL4SA and CL4SPY, the O...N distances are considerably short compared with other thermochromic *N*-salicylideneanilines. This shortening results, partly at least, from the substitution of chlorine atoms.

Firstly, we examined this substitution effect by means of MNDO calculations of the single molecules. Since all geometric parameters were fully optimized at a certain NH distance in these calculations, the optimized conformations might correspond to an isolated molecule, which is known to be nonplanar.¹¹⁾ The deformation of the hydrogen-bond structure due to this nonplanarity may be substantially small, because the major deformation from the planar conformation is a rotation of the aromatic ring at the aniline side. Therefore, the substitution effect is expected to appear to a large extent by this type of calculation. Figure 5 shows the results for CL4SA,

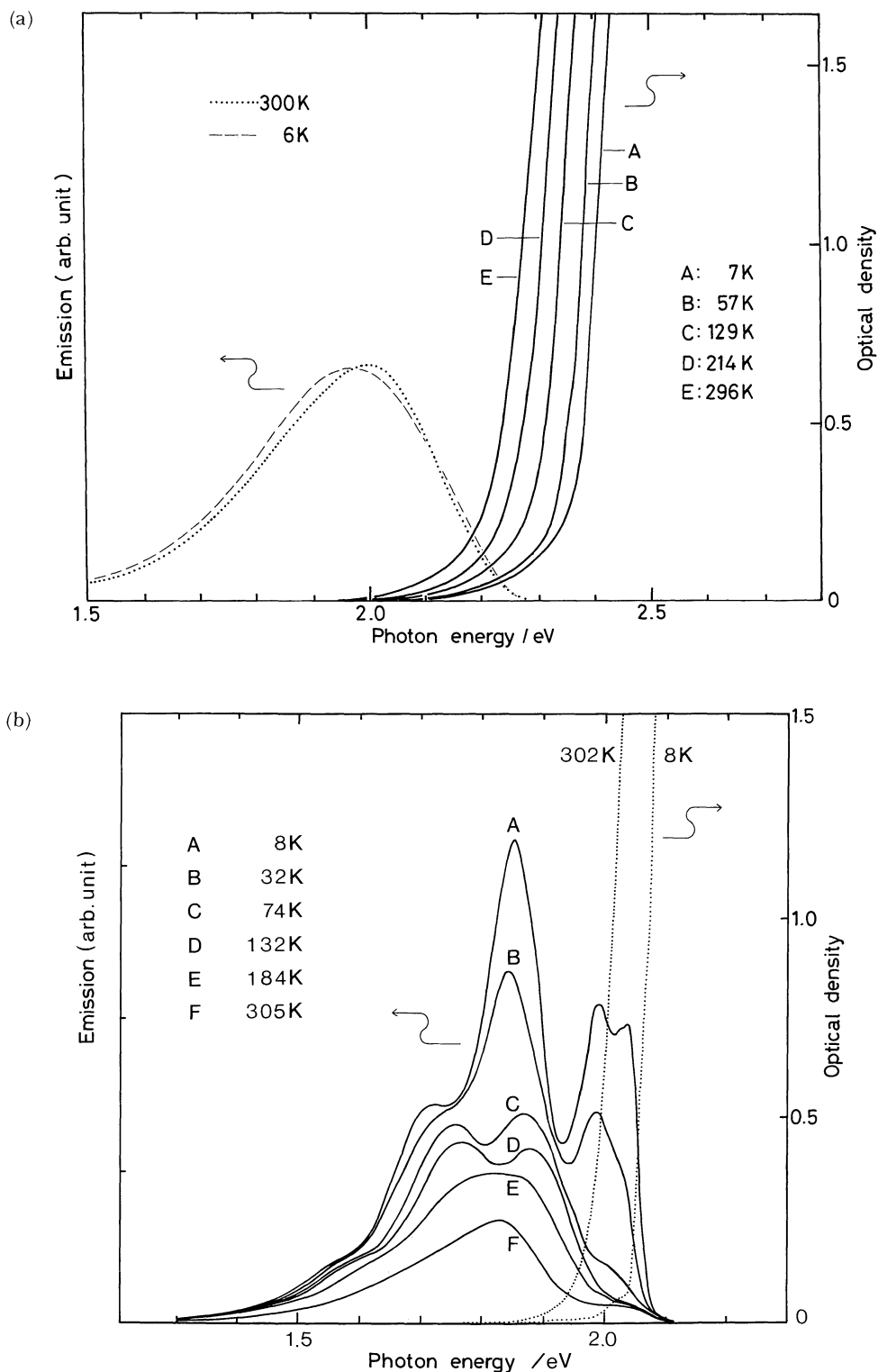
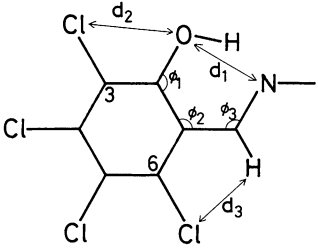


Fig. 4. Single-crystal absorption and emission spectral changes with temperature for CL4SA (a) and CL4SPY (b).

CL4SPY, and nonsubstituted *N*-salicylideneaniline. It can be seen that the space separation between two minima becomes smaller by the introduction of chlorine substituents. The energy difference between

the two minima is also smaller in chlorinated compounds. On the other hand, the difference between the aniline side structures, i.e., 1-pyrenyl and phenyl, has almost no influence on the potential

Table 5. Distances and Angles Related to the Steric Effect



	CL4SA		CL4SPY		<i>N</i> -salicylideneanilines ^{a)}	
	Obsd	Calcd ^{b)}	Obsd	Calcd ^{b)}	Obsd	Calcd ^{b)}
$d_1/\text{\AA}$	2.512(7)	2.84	2.534(5)	2.90	2.58—2.62	2.98
$d_2/\text{\AA}$	2.874(5)	2.90	2.902(4)	2.88	—	—
$d_3/\text{\AA}$	2.61(7)	2.40	2.59(3)	2.37	—	—
$\phi_1 + \phi_2 + \phi_3/^\circ$	361.4	371	362.8	373	364—367	376

a) Values for other derivatives which have no substituents at the 3 and 6 positions. b) Values obtained by MNDO calculations at the most stable conformation in Fig. 5.

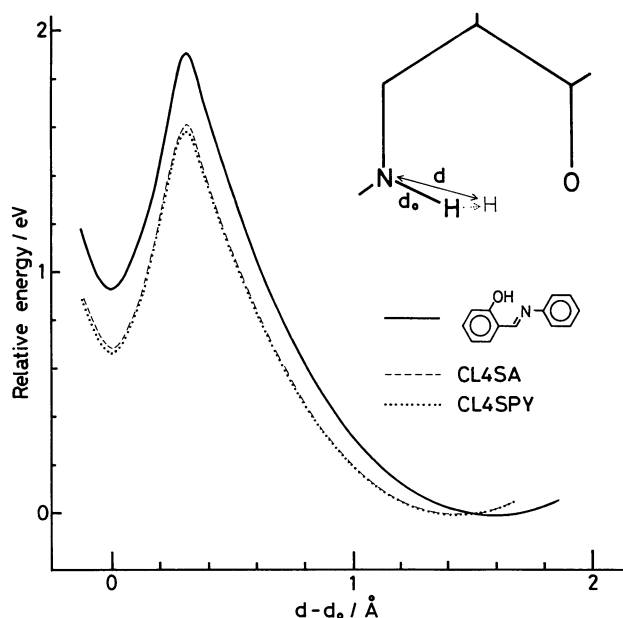


Fig. 5. Potential energy diagram calculated by an MNDO method. The energy is standardized at the OH form minima. The abscissa is the difference from the distance between N and H to that of the NH form minima.

surface of the proton.

The most notable effect of the chlorine substituents is considered to be a steric one; as shown in Table 5, the substituents at the 3 and 6 positions of the benzylidene side cause a contraction of the O...N distance due to a steric repulsion. A similar steric effect of the substituents on the hydrogen-bond structure was noticed in β -diketones¹²⁾ and salicylaldehydes.¹³⁾ Besides the steric effect, there might be an electronic effect of the substituents, as found for β -diketones.¹²⁾ However, in CL4SA and CL4SPY, this

effect is supposed to be negligibly small,¹⁴⁾ as far as single molecules are concerned. Consequently, the shortening of the hydrogen bond in CL4SA and CL4SPY can be considered to result from a steric effect of the chlorine substituents.

From the above arguments, CL4SA and CL4SPY should have the same strength as that of the hydrogen bond. The O...N distances are actually not so different in these two molecules. However, the spectroscopic studies for both crystals suggest that there is a substantial difference in the nature of the hydrogen bond in the crystalline state. It has also been noticed that the C(8)–O(5) distance of CL4SPY is considerably shorter than that of CL4SA. This indicates that the resonance contribution from the *o*-quinonoid structure in the NH form is larger in CL4SPY than in CL4SA. Although the N(6)–C(13) distance is also expected to be longer in CL4SPY than in CL4SA, this bond may not be so sensitive, due to a delocalization effect.

On the same basis, the observed optical properties can be interpreted as described below. Firstly, the intensity of the hydrogen stretching mode in these compounds may be considered to depend on the position of the hydrogen in the hydrogen bond. When the hydrogen vibrates near the center of the hydrogen bond, the induced dipole moment can be very weakly changed due to the delocalization of electrons in the entire chelate ring system.¹⁵⁾ Therefore, when the hydrogen-bond structure is closer to the intermediate one, the intensity becomes weaker.

Secondly, the temperature dependence of the visible absorption spectra must be considered. The thermochromic behavior is usually observed as a growth of new bands. When the energy difference between the thermochromic state and the thermal ground state is smaller or comparable to the thermal energy, the

thermochromic band has an appreciable intensity, even at low temperatures. Contrary to the case in BSP which shows a typical thermochromic-type behavior, the energy difference between the NH and OH forms is much smaller in both CL4SA and CL4SPY. This means that the content of the NH form is still large at the lowest temperatures in these measurements. Since the measurements were carried out by using single-crystal specimens, such intense absorption can hardly be observed as a clear peak. Thus, the initial growth or a peak profile of the thermochromic band could not be observed. In such a case, the approximate temperature dependence of the thermochromic band can be estimated from the shift of the absorption edge.¹⁶⁾ The relatively large shift in CL4SA indicates that the thermochromic band grows with increasing temperature, and this crystal can be regarded as being an ordinary thermochromic type. On the other hand, the smaller shift in CL4SPY in the same temperature range suggests that the growth approaches some degree of saturation. Such a situation is expected when the energy difference between the OH and NH forms is extremely small. The smaller Stokes shift compared with CL4SA also suggests a large contribution of the NH form in CL4SPY at low temperature.

From these structural and optical data, the energy difference between the two minima in the potential energy surface is considered to be much smaller in CL4SPY than in CL4SA. Considering the structural difference between the CL4SA and CL4SPY crystals, it is reasonable to assume that the intermolecular charge-transfer interaction operates in the CL4SPY crystal. This interaction is expected to make the ground state slightly polarized as a consequence of mixing with the excited state. Although this originates purely from a π - π interaction, it may cause a change in the net charge on the N and O atoms. Such an excess charge effect has been calculated and found to have great influence on the potential surface of the proton.¹⁷⁾

Since our interest lies in the influence on proton motion, we have tried to visualize the hydrogen in the

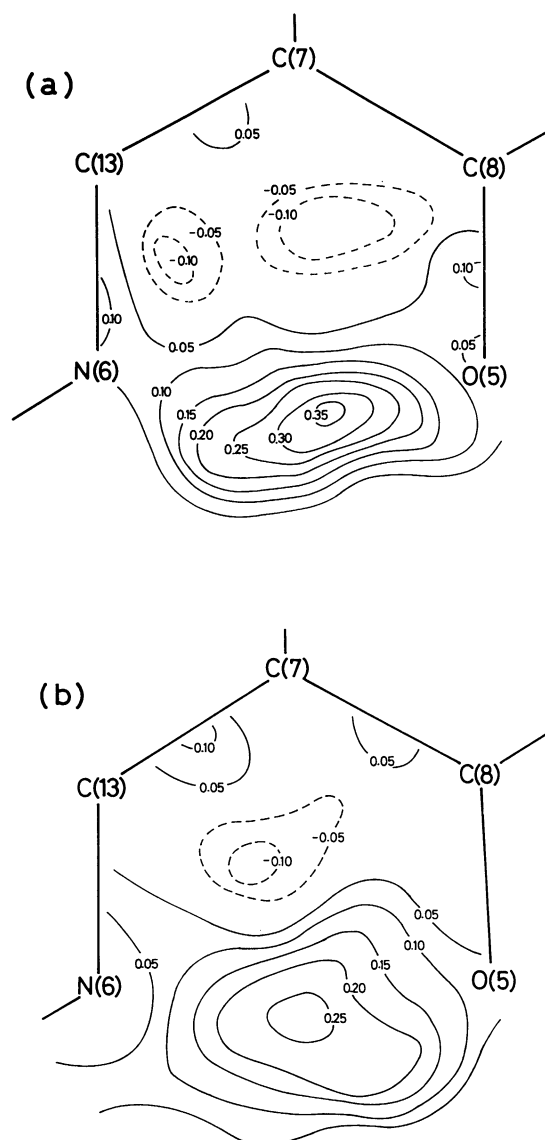


Fig. 6. Difference synthesis maps of the hydrogen bonded chelate ring ($e \text{ \AA}^{-3}$) of CL4SA (a) and CL4SPY (b).

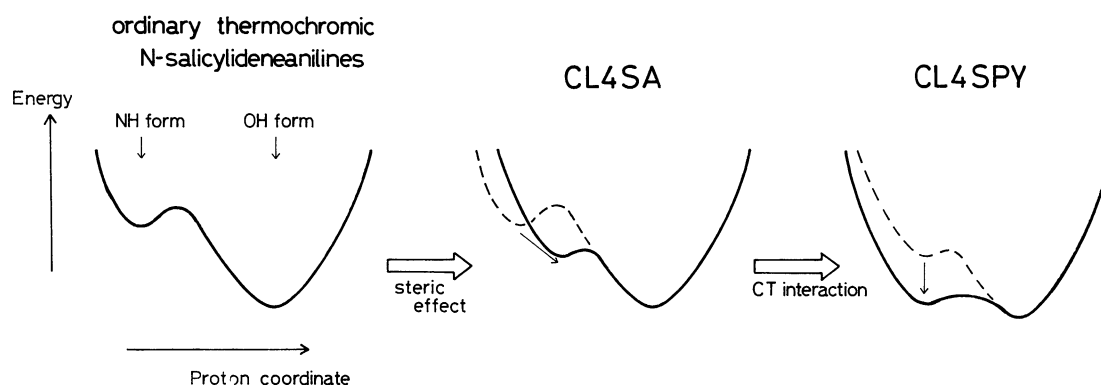


Fig. 7. Schematic representation of the potential energy surface of the proton modified by the steric effect and the intermolecular charge transfer (CT) interaction.

hydrogen bond. The method is the same as that performed for BSP and DSPY;⁹⁾ the difference syntheses are calculated by taking the parameters of the hydroxyl hydrogen out of the refined structure. The obtained electron-density maps are shown in Fig. 6. In both compounds, a broad peak appears at nearly the center of the hydrogen bond, which is quite different from the situation in ordinary thermochromic *N*-salicylideneanilines. The difference between CL4SA and CL4SPY may not be clearly seen due to the limitation of accuracy.

In conclusion, the strong hydrogen bonds in CL4SA and CL4SPY have mainly been attributed to a steric effect of the chlorine substituents at the 3 and 6 positions of the bezylidene side. In addition to this effect, the intermolecular charge-transfer interaction makes contribution from the NH form larger in CL4SPY, which makes the hydrogen-bond structure nearly intermediate between the NH and OH forms. These situations are schematically summarized in Fig. 7. The coupling between the proton transfer and the intermolecular π - π interaction may provide a hopeful prospect for the realization of the system proposed in the Introduction.

This work was partly supported by Scientific Research Grants-in-Aid No. 02804032 from the Ministry of Education, Science and Culture.

References

- 1) M. D. Cohen, G. M. J. Schmidt, and S. Flavian, *J. Chem. Soc.*, **1964**, 2041.
- 2) N. Hoshino, T. Inabe, T. Mitani, and Y. Maruyama, *Bull. Chem. Soc. Jpn.*, **61**, 4207 (1988).
- 3) T. Inabe, N. Hoshino, T. Mitani, and Y. Maruyama, *Bull. Chem. Soc. Jpn.*, **62**, 2245 (1989).
- 4) T. Inabe, submitted to *New J. Chem.*; T. Mitani, *Mol. Cryst. Liq. Cryst.*, **171**, 343 (1989).
- 5) H. Heaney, J. M. Jablonski, and C. T. McCarty, *J. Chem. Soc., Perkin 1*, **1972**, 2903.
- 6) P. Main, L. Lessinger, M. M. Woolfson, G. Germain, and J. -P. Declercq, MULTAN78, Univs. of York, England, and Louvain, Belgium (1978).
- 7) T. Sakurai and K. Kobayashi, *Rep. Inst. Phys. Chem. Res.*, **55**, 69 (1979).
- 8) The lists of structure factors, anisotropic thermal parameters for non-hydrogen atoms, and parameters for hydrogen atoms are deposited as Document No. 9102 at the Office of the Editor of *Bull. Chem. Soc. Jpn.*
- 9) J. Bregman, L. Leiserowitz, and K. Osaki, *J. Chem. Soc.*, **1964**, 2986.
- 10) J. Bregman, L. Leiserowitz, and G. M. J. Schmidt, *J. Chem. Soc.*, **1964**, 2068.
- 11) M. D. Cohen and S. Flavian, *J. Chem. Soc. B*, **1967**, 321.
- 12) J. Emsley, *Struct. Bonding*, **57**, 147 (1984), and references therein.
- 13) D. C. Nonhebel, *Tetrahedron*, **24**, 1869 (1968).
- 14) In the case of CL4SA or CL4SPY, both inductive and mesomeric effects of substituents are considered to be too small to change the electronegativities of the O and N atoms.
- 15) S. F. Tayyari, Th. Zeegers-Huyskens, and J. L. Wood, *Spectrochim. Acta, Part A*, **35**, 1289 (1979).
- 16) This behavior was confirmed by the measurements of BSP using a thick crystal or with increasing temperature well above room temperature.
- 17) M. Hasegawa, K. Daiyasu, and S. Yomosa, *J. Phys. Soc. Jpn.*, **28**, 1304 (1970).
- 18) C. K. Johnson, ORTEP, Report ORNL-3794, Oak Ridge National Laboratory, Tennessee (1976).